How Quickly Does a Hole Relax into an Engineered Defect State in CdSe Quantum Dots

Assaf Avidan,[‡,*] Iddo Pinkas,[†] and Dan Oron[‡]

[†]Department of Chemical Research Support, Weizmann Institute of Science, Rehovot, 76100 Israel, and [‡]Department of Physics of Complex Systems, Weizmann Institute of Science, Rehovot, 76100 Israel

ABSTRACT

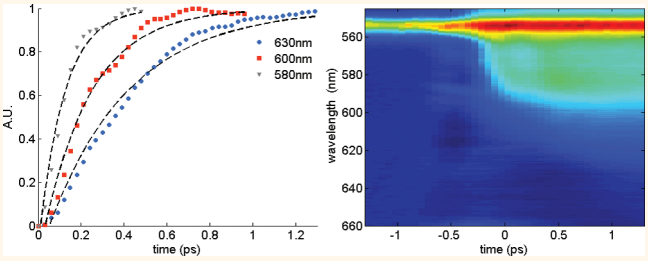

Intraband hole relaxation of colloidal Te-doped CdSe quantum dots is studied using state-selective transient absorption spectroscopy. The dots are excited at the band edge, and the defect band bleach caused by state filling of the hole is probed. Close to the defect energy, the hole relaxation is substantially slowed down, indicating a gap separating the defect state from the CdSe band edge. A clear dependence of the relaxation time with the QD's size is presented, implying that the hole relaxation is mediated by longitudinal optical (LO) phonon modes of the CdSe host. In addition, we find that overcoating the quantum dots by two monolayers of a ZnS shell extends the hole relaxation time by a factor of 2, suggesting a combined effect of LO phonons and surface effects governing intraband hole relaxation.

KEYWORDS: cooling · doping · holes · LO phonons · quantum dots

Colloidal semiconductor quantum dots (QDs) have many potential applications due to their appealing optical properties, which can be controlled by changing their size, shape, and material composition. The range of possible applications of QDs was extended recently by the ability to engineer built-in defects in several growth procedures.[1−6] In doped QDs, several atoms of the host material are replaced with dopants, potentially leading to changes in the energetic spectrum of the particles by creating new electron/hole energy levels inside the host gap. Such impurities are often used to manipulate various properties in desirable and controllable ways, addressing key application problems and practically introducing a new class of functional materials. For example, doping can be used to improve the QDs' thermal properties[7] or to control band alignment,[8] thus making them more suitable for various applications.[9] In the context of optical gain, it can be used to remove the exciton/biexciton degeneracy which suppresses optical gain in CdSe QDs.[5] Although various dopant materials were already successfully incorporated into II−VI QDs, a well founded basic description of the carrier dynamics inside these materials is missing. In particular, this is the case for the dynamics of intraband carrier cooling from the host to the defect state.

In bulk semiconductors, the energy spectrum of the electrons and holes is dense enough so that electron−phonon coupling is the dominant intraband charge relaxation mechanism, leading to ∼1 eV/ps relaxation rates.[10,11] However, the density of states of semiconductor QDs is size-dependent, and in the strong confinement regime, the spacing between the energy levels can reach hundreds of millielectronvolts, way above the LO phonon energy. As a result, it was initially predicted that intraband phonon relaxation rates in QDs will be substantially lower than in bulk materials.[12,13] Surprisingly, femtosecond pump−probe experiments showed that in the conduction band the 1P → 1S electron relaxation rate in CdSe QDs is similar to the intraband relaxation rates found in bulk materials.[11,14,15] To explain this discrepancy, it was theoretically proposed[16] and experimentally verified[13,17,18] that electron cooling in QDs is governed by an Auger-type mechanism, where the electron cools down to the 1S conduction state by transferring its energy to phonons *via* Coulomb interaction with the hole.

Intraband hole relaxation was also discussed extensively in the literature, and was found to be dominated by several relaxation mechanisms.[19] In particular,

* Address correspondence to avidan.assaf@gmail.com.

Received for review December 2, 2011 and accepted March 22, 2012.

Published online March 22, 2012
10.1021/nn204690p

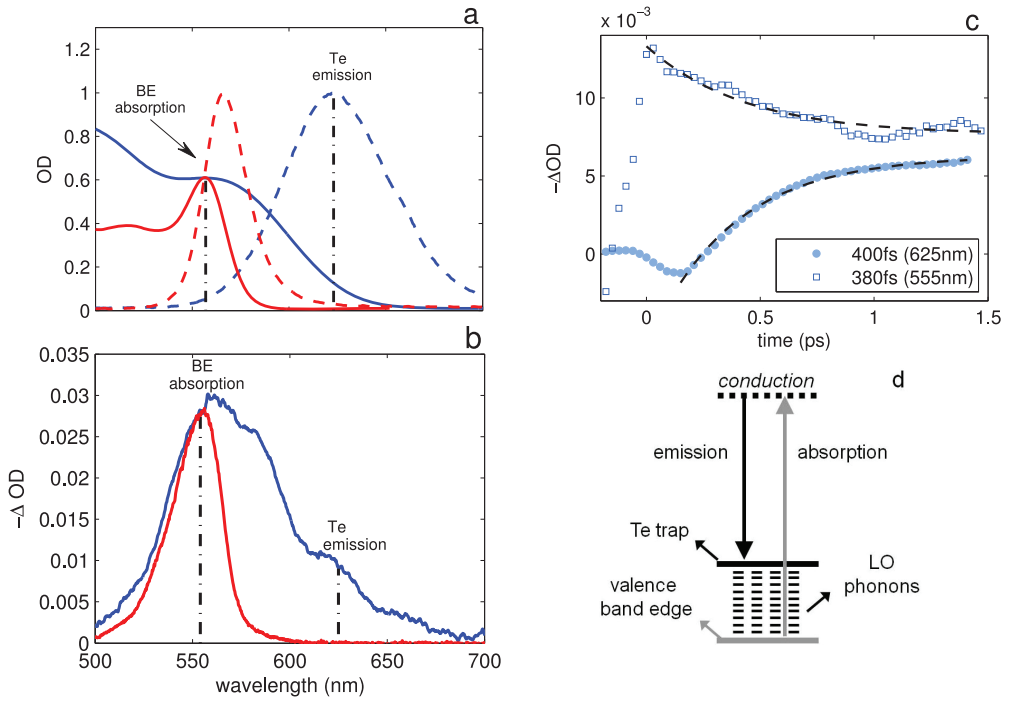

Figure 1. Linear and nonlinear absorption and TA dynamics of CdSe:Te QDs. (a) Linear absorption spectrum (blue) and photoluminescence emission of CdSe:Te (dashed blue) dots with a radius of R = 1.7 nm. The band edge (BE) exciton wavelength and the emission maximum wavelength are marked with a dash-dot vertical line. (b) Transient absorption spectrum of the same dots presented in (a) recorded 2 ps after excitation. The doped particles are shown in solid blue and the undoped in red. (c) Chirp-free population dynamics at the BE transition wavelength (empty blue squares) and at the Te trap (blue circles). Note the complementary dynamical behavior of the BE and the Te trap state. (d) Energy diagram showing the hole route from the CdSe valence host to the Te trap. Note: the horizontal axis of (a) is identical to (b) but was removed for convenience.

three mechanisms were experimentally investigated including both adiabatic and nonadiabatic phonon-assisted relaxation[14,15,20,21] as well as charge relaxation *via* surface states. Since the hole effective mass in CdSe QDs is approximately three times larger than that of the electron, an Auger-dominated cooling is improbable for holes. Cooney *et al.*[20] showed that the 2S → 1S hole relaxation is size-independent in CdSe QDs, due to nonadiabatic phonon relaxation which balances the adiabatic LO Frohlich interaction. Earlier it was found[15] that for CdSe QDs the temporal onset of the band edge emission, at different energetic distances from a constant pump pulse, is divided into fast and slow regimes. This was later explained theoretically[22] by intraband energy gaps slowing down the hole adiabatic relaxation process. In addition, surface passivation using a thick shell of ZnS resulted in a longer relaxation time, which suggests charge relaxation through surface states.[20] As mentioned earlier, these experiments suggest that hole relaxation in II−VI semiconductor QDs is not dominated by a single process but is rather controlled by the interplay of several relaxation channels through which intraband hole relaxation occurs.

In this paper, we extend the study to doped QDs and look at a particular system which enables us to engineer a single isolated defect state within the host energy gap, into which the valence band edge hole relaxes. Doped QDs have recently been the subject of intense study[1] but were not studied in the context of charge carrier cooling. In view of their possible applications, it is interesting to study the fundamental photophysics of doped dots and, in particular, intraband charge carrier relaxation pathways in doped semiconductor QDs. The simplest case of doped QDs is described by a single isolated energy state within the energy gap of the host.

Our dots are regular CdSe QDs doped with Te atoms (CdSe:Te). In these particles, a small cluster of CdTe (less than 5 atoms) is formed at the early stages of the synthesis,[5] over which CdSe is grown. As was shown in previous experiments,[5] a spatially localized trap state is formed within the dot which localizes the hole wave function.[5,6] Since Te and Se atoms have the same electronic configuration in the two outer shells, Te doping is isovalent, meaning that it should not change the Fermi level of the dot.[8] However, since a Te atom has more shells populated with higher electronic levels compared with Se atoms, when incorporated inside a CdSe QD, a populated electron energy level is created above the CdSe valence band edge. Upon excitation at the band edge, the hole created at the CdSe valence band edge quickly relaxes to the Te trap where it radiatively recombines with the conduction band electron (see Figure 1d). The spatial trap state localizing the

hole implies a reduced overlap with the electron wave function and thus a stronger polarization of the host atoms, which induces a large coupling to high energy LO phonon modes.[23] It is thus expected that intraband charge carrier relaxation dynamics will show significant dependence on the QDs size. The decay mechanism and the characteristic cooling time of the hole to the Te defect and its size dependence are at the focus of this work. This system enables us to study hole cooling in the presence of an already cold electron as well as to control the energetic shift of the trap state from the valence band edge by changing the QD size. Thus, it is possible to isolate the hole dynamics and characterize it as a function of the amount of energy lost in the cooling process.

We adopt the state-selective transient absorption approach, recently presented by Cooney *et al.*[21] Since the Stokes shift in CdSe:Te QDs is significantly larger compared with that of undoped CdSe QDs (see Figure 1a), it is possible to probe the hole population directly at the emission band without being affected by the strong excitation beam. Upon photoexcitation at the band edge, the electron populates only the lowest ($1S_e$) state at the conduction band, and the dynamics is entirely dominated by the hole. By identifying a complementary dynamical behavior between the band edge and the defect state populations, we find that hole trapping happens on a subpicosecond time scale. In addition, we examine the size dependence of the relaxation rate and show that the trapping time decreases when increasing the dot's size. The effect of surface states on the relaxation rate was examined by coating the dots with a thin shell (two monolayers) of ZnS, leading to a longer relaxation time. As will be explained below, these findings suggest a combined relaxation mechanism involving LO phonons and surface traps.

RESULTS AND DISCUSSION

Measurements were preformed in the usual pump–probe configuration. An 800 nm Ti:sapphire amplifier is used to pump an optical parametric amplifier (OPA) which produces a wavelength tunable (500–700 nm) source with pulse duration of 120 fs at a repetition rate of 1 kHz. This pulse is followed by a white light continuum pulse, generated by focusing part of the 800 nm beam onto a 3 mm sapphire plate. At each step, we take consecutive measurements with (α) and without (α_0) the pump, and the relative absorption $\Delta\alpha = \alpha - \alpha_0$ is obtained. We use a clear toluene solution of precipitated CdSe:Te QDs which were vigorously stirred throughout the measurements. The power level at each experiment is maintained low enough (number of excitations per dot per pulse is less than half) in order to avoid fast multiexciton dynamics. In Figure 1a, we plot the linear absorption spectrum of the CdSe:Te particles (solid blue line) and on top the absorption spectrum of regular CdSe QDs synthesized by using a similar synthetic protocol but without addition of Te. The CdSe:Te QDs have a broader band edge onset relative to the undoped particles and a broad Stokes shifted (centered at 625 nm) photoluminescence (PL) emission spectrum.[5] The Stokes shift of the emission is due to a Te energy level inside the gap of the CdSe host (see Figure 1d), created by the Te dopant.

The band edge absorption of the dots is the first local maximum of the absorption spectrum (marked with an arrow in Figure 1a). Moreover, we assume that the band edge excitation of the CdSe:Te QDs involves only excited states of the holes. This is especially true in our case since the Se and Te atoms have a similar ground state electronic configuration. Thus, if we assume that the conduction band of the CdSe:Te QDs is unaffected by the Te replacement,[6] the next electronic transition is about 0.35 eV from the conduction edge (for a dot with $R = 2$ nm). In order not to populate higher conduction states, in each experiment, we tune the excitation wavelength to the band edge exciton.

A typical transient absorption spectrum of CdSe:Te QDs utilizing band edge excitation is shown in Figure 1b. The effect of the Te doping element is evident by comparing the chirp-corrected transient absorption spectra of the doped sample (Figure 1b, blue solid line) and of undoped CdSe particles (red line) at about 2 ps after excitation. The transient absorption spectrum of the doped dots is much broader, extending to the red far beyond the main exciton bleach band, revealing additional bleach bands, which are assigned to the Te defect. The lobe at 625 nm coincides with the center of the PL emission. The additional bands centered at 585 and 660 nm (also marked with dashed line in Figure 1b) are resolved only in the transient absorption spectrum (not in the absorption or PL spectra) and are clearly resultant from the Te defect. Since the nature of this broadening is not known, in what follows, we address only the peak that overlaps with the emission maximum of the PL spectrum.

In Figure 1c, we plot the dynamics probed at the excitation wavelength (open blue squares) and at the center of the emission (solid blue circles). The defect state dynamics shows a delayed rise preceded by a small dip resulting from induced absorption due to the band edge population. This recovery from induced absorption to bleach is the result of state filling of the defect and is a bleach signal caused by the small defect absorption band. The band edge population rises instantaneously $\tau_{BE} < 180$ fs and follows a decay with an amplitude and time constant matching the dynamics probed at the emission wavelength. This complementary behavior is robust and has appeared in all of the doped samples we have measured. In order to quantitatively evaluate the defect state bleach band

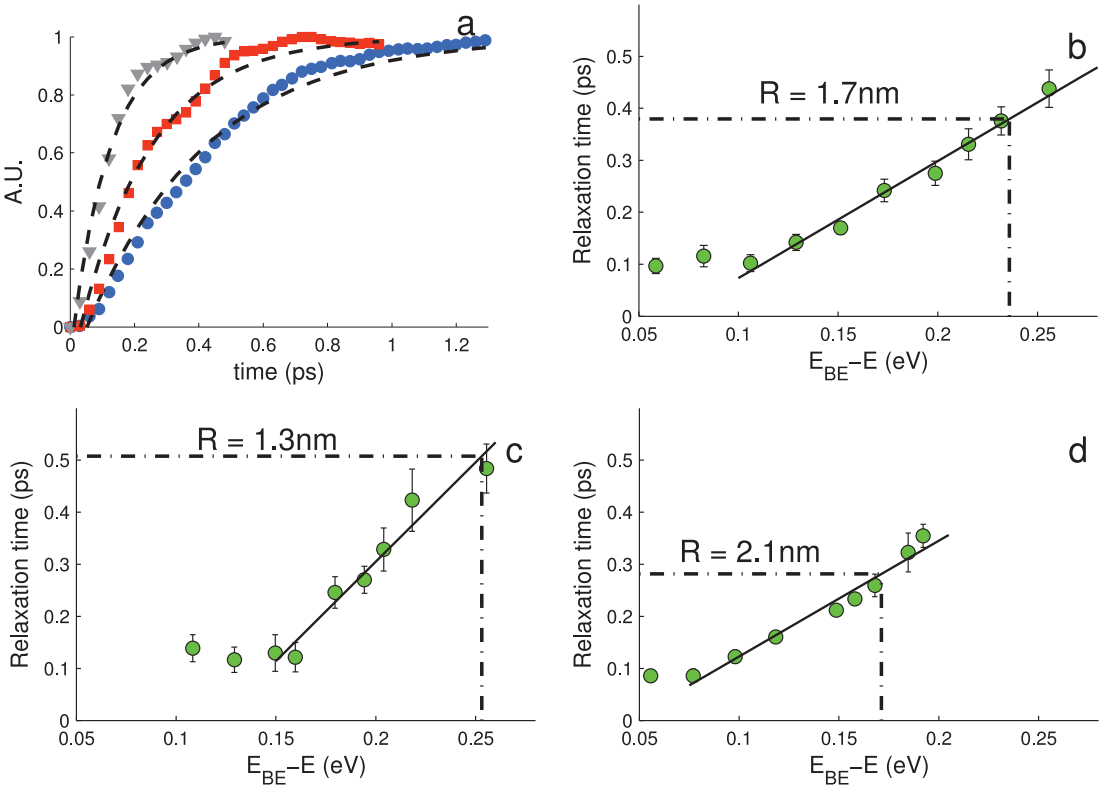

Figure 2. (a) Rising population at $E_{BE} - E = 80$ meV (gray triangles), 170 meV (red squares), and 255 meV (blue circles) for the intermediate size sample ($R = 1.7$ nm). (b–d) Inspection of the defect bleach band rise time across the TA spectrum, for three dot sizes extracted from the same synthesis. The green circles represent time constants obtained from a rising exponent best fit with 95% confidence bounds. The black line is a linear fit to the increasing part of the plot. The buildup time of the defect bleach band is extracted by obtaining the value of the fit at the energy corresponding to the maximum of the PL emission spectrum (dash-dot line in plots b–d). The *x* and *y* scales in (b–d) are the same.

dynamics, we have fitted the data to an exponential function with a single time constant. In the figure, we plot (in dashed black line) the fit of the function $a\ (1 \mp \exp^{-t/\tau})$ to both the rise of the bleach signal at the defect ($\tau = 380$ fs minus sign) and to the decaying part of the band edge bleach signal ($\tau = 400$ fs plus sign). A similar time constant is found, which strongly suggests that the two signals are correlated. Such a fast relaxation time was also observed in previous experiments measuring hole dynamics.[14,20]

Next we examine the size dependence of the characteristic relaxation time to the defect as described above. Since we have found that the defect relaxation time slightly changes between syntheses, we have performed the measurements on samples which were extracted from the same synthesis. The size of each sample was determined according to the extinction coefficient size scaling presented by Yu *et al.*[24] for CdSe QDs. Figure 2b shows an inspection of the defect bleach band time constant at each energetic distance from the band edge energy, for the intermediate size sample ($R = 1.7$ nm). The points on the figure are obtained by the following procedure: We extract from the time trace of the TA spectrum the relaxation constant at energies E (see Supporting Information[26] for the data analysis procedure), spreading from the band edge energy to the energy corresponding to the center of the PL emission. The decaying exponent of each energy is plotted against $E - E_{BE}$, where E_{BE} is the band edge exciton absorption energy. As was stated above, each curve was fitted (black dashed line) to an exponential function with a single time constant with confidence bounds of 95%.

Examples of the fits are shown in Figure 2a, where the population dynamics for three different energies across the TA spectrum of the sample mentioned above is presented.[26] In the figure, we plot in blue circles the dynamics close to the defect emission center corresponding to $E - E_{BE} = 255$ meV in Figure 2b, in red squares the dynamics corresponding to $E - E_{BE} = 170$ meV, and in gray triangles the dynamics corresponding to $E - E_{BE} = 80$ meV (close to the band edge excitation). Figure 2b shows that the hole relaxation is composed of two spectral regimes. For energies less than about 100 meV, the rise is instantaneous (system response[26] is 180 fs), and above this energy, the rise time increases linearly. Such a behavior was also observed in an earlier experiment[14] probing intraband hole relaxation in CdSe QDs through transient emission measurements. In order to have a more accurate evaluation of the characteristic time of the defect bleach dynamics, we fit a linear line to the increasing

part of the data in Figure 2b. This way we minimize the error in extracting the relaxation time constant at the energy which corresponds to the difference between the BE energy and the peak of the PL spectrum.

Using the same procedure, we have analyzed the defect bleach rise time for the other two samples obtained from the synthesis. All sample sizes show a very similar qualitative dynamical behavior (see Figure 2b–d), namely, a constant regime where the relaxation time is approximately the system response and a regime where the decay time increases linearly. The relaxation times found are subpicosecond, in agreement with previous TA experiments which measured hole dynamics in CdSe QDs.[14,15,20] The data present a small inverse dependence of the relaxation time on the size of the nanocrystals. The largest dot (R = 2.1 nm) has the shortest (0.29 ps) relaxation time and *vice versa*. Because of technical system limitation, the excitation wavelength of the smallest sample is 45 meV above the band edge absorption (535 nm instead of 525 nm), so that the true relaxation time is expected to be longer than the one found in experiment (larger than 0.5 ps). The same is true for the largest sample where we pump at 582 nm instead of 588 nm, where the relaxation constant is expected to be lower than the value obtained in experiment (smaller than 0.29 ps). The size dependence of the hole relaxation time in our experiment is surprising, especially in view of previous experiments employing initial state selectivity.

The size dependence of the relaxation time is presented in Figure 3, where we plot the relaxation time as a function of both the QD radius and the Stokes shift. There is a clear scaling between the relaxation time and the energetic distance between the absorption and PL emission maximum. The error bars along the *y*-axis (relaxation time) are derived from the error bars in Figure 2b–d, and along the *x*-axis are just the error of assigning the PL maximum and the band edge exciton energy. Although the relaxation times are still very short, the scaling clearly shows that a larger intraband energy gap slows down phonon-assisted cooling.[11,14] Moreover, this trend implies that the final stage of the hole relaxation is slowed down by a small density of states or an intraband gap[22] separating the valence edge of the energy spectrum from the Te defect state.

Another important parameter is the rate of energy dissipation dE/dt, which can be extracted from Figure 2b–d, by obtaining the slope of each linear fit presented in the figure. The results are 0.45 ± 0.035, 0.39 ± 0.03, and 0.26 ± 0.025 eV/ps for the dot radii R = 2.1, 1.7, and 1.3 nm, respectively (values in parentheses are the standard deviation error bars derived from the fits). It is interesting to note that dE/dt ∝ R. Smaller dots have a smaller LO phonon density of states, and as a result, their energy dissipation rate is smaller than for larger dots. This result confirms the central role that LO phonons have regarding hole cooling in doped QDs.

We have also examined the effect of the surface on the hole dynamics. Whereas surface effects were shown to dominate the electron relaxation[25] from the 1P → 1S levels, the surface influence on the hole

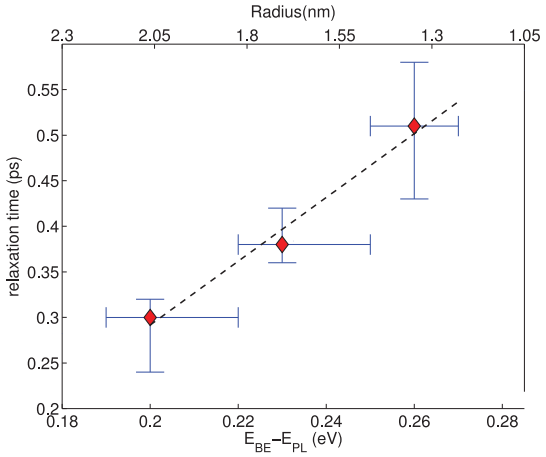

Figure 3. Relaxation time constant as a function of the Stokes shift and of the dot radius. The three points correspond to the three different dot sizes, where the longest relaxation time corresponds to the smallest dot.

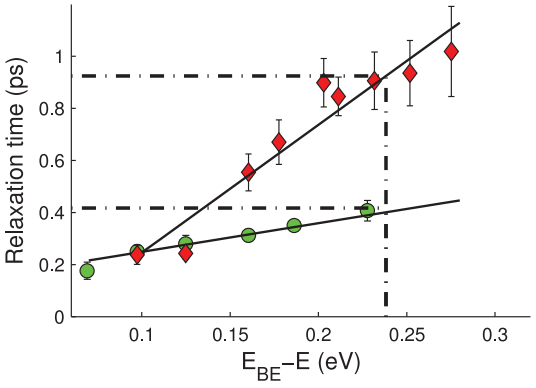

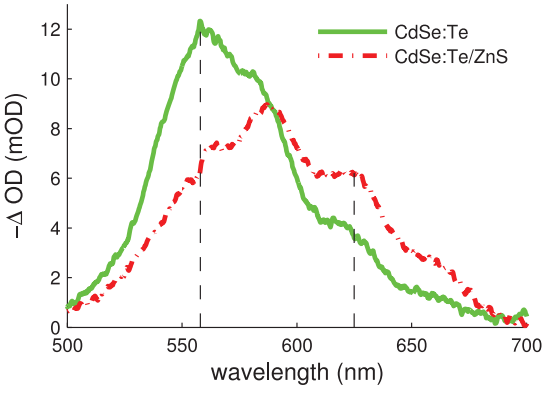

Figure 4. Comparison between the hole relaxation time of the CdSe:Te QDs and CdSe:Te/ZnS (with two ZnS monolayers) QDs. Right plot: Chirp-corrected TA spectrum of CdSe:Te QDs (green solid) and of CdSe:Te/ZnS with two monolayers of ZnS (dash-dot red), 2 ps after excitation. Left plot: Relaxation time of the two samples as a function of the energy distance from the band edge exciton. The ZnS passivated sample (red diamonds) clearly shows slower dynamics.

relaxation mechanism still needs to be accounted for.[14,15,20] We used a zinc diethyldithiocarbamate as a single source precursor to overcoat a CdSe:Te R = 1.7 nm QD with two monolayers of ZnS. New CdSe:Te QDs were prepared for this task by applying the same synthesis described previously. A comparison between the TA spectrum of CdSe:Te (green solid) and the coated CdSe:Te/ZnS QDs (dash-dot red) is presented in the right plot in Figure 4. The excitation and emission lines of the dots are marked with vertical lines at 558 and 625 nm. The band edge absorption line and the emission line of the CdSe:Te/ZnS QDs are slightly red-shifted compared to the CdSe:Te dots, due to the shell growth. The ZnS layers form a large potential barrier separating the hole wave function from the surface ligands. As a result, the relaxation rate is suppressed by a factor of 2, where in the ZnS-capped QDs we find a relaxation time of nearly 1 ps compared to 0.4 ps measured on the same dot before it was coated. Thus, although the hole is localized to the Te defect, it is still greatly affected by the CdSe surface.

CONCLUSIONS

To conclude, we have measured hole relaxation from the band edge to the Te state in CdSe:Te QDs. The state-selective excitation enables us to focus on the hole dynamics and isolate it from electron contributions in the conduction band. The results suggest that two different mechanisms dominate the hole dynamics. The first is LO phonon-assisted relaxation, a process in which the relaxation time of the hole from the CdSe band edge to the Te defect increases substantially when approaching the emission maximum wavelength. This same behavior was reported by Xu *et al.*[14] and was later explained theoretically[22] by energy gaps within the valence band created by the fine structure of the valence band. In our dots, an energy gap which separates the Te defect from the valence edge slows down the hole intraband relaxation, as is shown in Figure 2b–d. The size dependence found also suggests the involvement of LO phonons since it directly correlates the energetic Stokes shift with the relaxation time. This result was also observed by Xu *et al.*;[14] however, the excitation used in that experiment was fixed (400 nm, the same for all sample sizes), and higher conduction states are not ideally excluded from the relaxation process. Size scaling was also found for the rate of energy dissipation. This finding further strengthens the conclusion that LO phonons are taking part in the hole relaxation to the Te defect in CdSe:Te QDs. However, LO phonons alone cannot explain the subpicosecond relaxation rates observed. Thus, another mechanism must participate in the process. We find evidence that surface effects have a strong influence on the relaxation time, despite the fact the final hole state is highly localized inside the dot. The same dots only covered with two monolayers of ZnS showed a much longer hole relaxation time constant (0.9 ps for ZnS covered dots, 0.4 ps for uncovered dots). Our results show rich photophysics and intraband dynamics of excited carriers in Te-doped CdSe QDs and suggest ways for manipulating intraband dynamics to better control and extend the hole relaxation time through the incorporation of dopant atoms inside II–VI semiconductor QDs.

MATERIALS AND METHODS

CdSe:Te Sample Preparation. To produce CdSe:Te, we follow a synthesis previously published.[5] First, 26 mg of CdO and 120 mg of tetradecylphosphonic acid are mixed in a three-neck 50 mL flask, dissolved in 8 mL of octadecene (ODE), and brought to 300 °C under an inert atmosphere. In a separate container, 15 mg (0.2 mM) of selenium powder are dissolved in 4 mL of trioctylphosphine (TOP), to which 0.01 mM tellurium powder is added. The TOP:Se/Te solution is ultrasonicated until it is clear and is then swiftly injected to the hot flask. While the reaction is taking place, we extract several samples of increasing size. Finally the CdSe:Te QDs are precipitated using toluene and acetone/methanol for further inspection.

ZnS Overshell Growth. To overcoat the CdSe:Te dot with ZnS, we use zinc diethyldithiocarbamate as a single source precursor dissolved in TOP at a concentration of 0.1 M. The precipitated CdSe:Te sample (0.05 μM) is dissolved in 1 mL of TOP (with 200 μL of chloroform) and is added to a flask containing 4 mL of ODE, 1.8 g of octadecylamine, and 1 mL of hexadecylamine. This mixture is left under vacuum at 120 °C for about an hour. The temperature is then raised to 150 °C under inert atmosphere, and the ZnS precursor is added dropwise while the temperature is slowly raised to 200 °C. To prepare the ZnS precursor, we dissolve the zinc diethyldithiocarbamate precursor in oleylamine at 0.1 M. The quantity of the ZnS precursor injected was calculated using the size scaling curve of undoped CdSe presented in the work of Yu *et al.*[24]

All chemicals were purchased from Sigma Aldrich.

Conflict of Interest: The authors declare no competing financial interest.

Acknowledgment. This research was supported by the European Research Council starting investigator grant SINSLIM 258221 and by the Crown center of photonics. D.O. is the incumbent of the Recanati career development chair of energy research.

Supporting Information Available: Additional experimental details and figures. This material is available free of charge *via* the Internet at http://pubs.acs.org.

REFERENCES AND NOTES

1. Norris, D. J.; Efros, A. L.; Erwin, S. C. Doped Nanocrystals. *Science* **2008**, *319*, 1776–1779.
2. Norris, D. J.; Yao, N.; Charnock, F. T.; Kennedy, T. A. High Quality Manganese-Doped ZnSe Nanocrystals. *Nano Lett.* **2001**, *1*, 3–7.
3. Pradhan, N.; Goorskey, D.; Thessing, J.; Peng, X. An Alternative of CdSe Nanocrystals Emitters: Pure and Tunable Impurity Emission in ZnSe Nanocrystals. *J. Am. Chem. Soc.* **2005**, *127*, 17586–17587.
4. Pradhan, N.; Peng, X. Efficient and Color Tunable Mn-Doped ZnSe Nanocrystal Emitters: Control of Optical Performance *via* Greener Synthetic Chemistry. *J. Am. Chem. Soc.* **2007**, *129*, 3339–3347.

5. Avidan, A.; Oron, D. Large Blue Shift of the Biexciton State in Tellurium Doped CdSe Colloidal Quantum Dots. *Nano Lett.* **2008**, *8*, 2384–2387.
6. Franzl, T.; Müller, J.; Klar, T. A.; Rogach, A. L.; Feldmann, J.; Talapin, D. V.; Weller, H. CdSe:Te Nanocrystals: Band Edge *versus* Te-Related Emission. *J. Phys. Chem. C* **2007**, *111*, 2974–2979.
7. Menkara, H.; Gilstrap, R. A.; Morris, T.; Minkara, M.; Wagner, B. K.; Summers, C. J. Developement of Nanophosphores for Light Emitting Diodes. *Opt. Express* **2011**, *19*, A972–A981.
8. Mocatta, D.; Cohen, G.; Schattner, J.; Millo, O.; Rabani, E.; Banin, U. Heavily Doped Semiconductors Nanocrystals Quantum Dots. *Science* **2011**, *332*, 77–81.
9. Beaulac, R.; Archer, P. I.; Ochsenbein, S. T.; Gamelin, D. R. Mn-Doped CdSe Quantum Dots: New Inorganic Materials for Spin Electronics and Spin-Photonics. *Adv. Funct. Mater.* **2008**, *18*, 3873–3891.
10. Conwell, E. *High Field Transport in Semiconductors*; Academic Press: New York, 1967.
11. Klimov, V. I. Optical Nonlinearities and Ultrafast Carrier Dynamics in Semiconductor Nanocrystals. *J. Phys. Chem. B* **2000**, *104*, 6112–6123.
12. Bockelmann, U.; Bastard, G. Phonon Scattering and Energy Relaxation in Two-, One-, and Zero-Dimensional Electron Gases. *Phys. Rev. B* **1990**, *42*, 8947–8951.
13. Klimov, V. I.; McBranch, D. W.; Leatherdale, C. A.; Bawendi, M. G. Electron and Hole Relaxation Pathways in Semiconductor Quantum Dots. *Phys. Rev. B* **1990**, *60*, 13740–13749.
14. Xu, S.; Mikhailovsky, A. A.; Hollingsworth, J. A.; Klimov, V. I. Hole Intraband Relaxationin Strongly Confined Quantum Dots: Revisiting the Phonon Bottleneck Problem. *Phys. Rev. B* **2002**, *70*, 045319(1−5).
15. Klimov, V. I.; Schwarz, Ch. J.; McBranch, D. W.; Leatherdale, C. A.; Bawendi, M. G. Ultrafast Dynamics of Inter- and Intraband Transitions in Semiconductor Nanocrystals: Implications for Quantum-Dot Lasers. *Phys. Rev. B* **1999**, *60*, R2177–R2180.
16. Efros, A. L.; Kharchenko, V. A.; Rosen, M. Breaking the Phonon Botlleneck in Nanometer Scale Quantum Dots: Role of Auger-Like Processes. *Solid State Commun.* **1995**, *93*, 281–284.
17. Klimov, V. I.; Michailovski, L. L.; McBranch, D. W.; Leatherdale, C. A.; Bawendi, M. G. Mechanisms for Intraband Energy Relaxation in Semiconductor Quantum Dots: The Role of Electron−Hole Interactions. *Phys. Rev. B* **2000**, *61*, 13349–13352.
18. Hendry, E.; Koeberg, M.; Wang, F.; Zhang, H.; de Mello Donega, C.; Vanmaekelbergh, D.; Bonn, M. Direct Observation of Electron-to-Hole Energy Transfer in CdSe Quantum Dots. *Phys. Rev. Lett.* **2006**, *96*, 057408(1−4).
19. Kambhampati, P. Hot Exciton Relaxation Dynamics in Semiconductor Quantum Dots: Radiationless Transitions on the Nanoscale. *J. Phys. Chem. C* **2011**, *115*, 2208922109.
20. Cooney, R. R.; Sewall, S. L.; Anderson, K. E. H.; Dias, E. A.; Kambhampati, P. Breaking the Phonon Bottleneck for Holes in Semiconductor Quantum Dots. *Phys. Rev. Lett.* **2007**, *98*, 177403(1−4).
21. Cooney, R. R.; Sewall, S. L.; Dias, E. A.; Sagar, D. M.; Anderson, K. E. H.; Kambhampati, P. Unified Picture of Electron and Hole Relaxation Pathways in Semiconductor Quantum Dots. *Phys. Rev. B* **2007**, *75*, 245311(1−14).
22. Califano, M.; Bester, G.; Zunger, A. Prediction of a Shape-Induced Enhancement in the Hole Relaxation in Nanocrystals. *Nano Lett.* **2003**, *3*, 1197–1202.
23. Nomura, S.; Kobayashi, T. Exciton-LO-Phonon Couplings in Spherical Semiconductor Nanocrystals. *Phys. Rev. B* **1992**, *45*, 1305–1316.
24. William, W. Yu.; Lianhua, Q.; Wenzhuo, G.; Peng, X. Experimental Determination of the Extinction Coefficient of CdTe, CdSe, and CdS Nanocrystals. *Chem. Mater.* **2003**, *15*, 2854–2860.
25. Pandey, A.; Guyot-Sionnest, P. Slow Electron Cooling in Colloidal Quantum Dots. *Science* **2008**, *322*, 929–932.
26. System response is obtained by taking the solvent response, which is as short as 180 fs; see Supporting Information.